Journal of the European Ceramic Society **11** (1993) 133–141

Static and Cyclic Fatigue of 2Y-TZP Ceramics with Natural Flaws

Tianshun Liu,* Ralf Matt & Georg Grathwohl

Institut fuer Keramik im Maschinenbau, Universitaet Karlsruhe, Haid-und-Neu-Strasse 7, D-7500 Karlsruhe, Germany

(Received 13 February 1992; revised version received 9 April 1992; accepted 3 July 1992)

Abstract

Static and cyclic fatigue properties of two 2Y-TZP ceramics with average grain sizes of 0·2 and 1·6 μm were studied in bending tests. A large number of specimens with natural flaws were used for the measurement of the initial strength distribution and for the static and cyclic fatigue (stress ratios $R = 0{\cdot}2$ and -1) tests at a single maximum stress level. From these experimental data the modified stress–life time (σ–t_f) curve and the crack propagation relation (da/dt–K_I curve) can be calculated using both the fracture mechanics and the statistical approaches. It was found that the measured time to failure under cyclic loadings, especially with the stress ratio of -1, is much shorter than under static loadings. The crack growth relation for the natural flaws can be described by the power law function $da/dt = AK_I^n$. Fatigue crack velocities under cyclic loadings are much higher than those under static loading at the same stress intensity. A significant cyclic fatigue effect can be concluded for the 2Y-TZP materials. Besides this cyclic fatigue effect a strengthening effect was also found for the survivor specimens after static and cyclic loading which is believed to be due to a modification of the initial flaws during the long term fatigue loadings.

Die Ermüdungseigenschaften für statische und zyklische Beanspruchung zweier 2Y–TZP-Keramiken mit einer Durchschnittskorngröße von 0·2 und 1·6 μ wurden mittels Biegeversuche untersucht. Eine große Anzahl Proben mit natürlichen Fehlern wurde zur Messung der Ausgangsfestigkeitsverteilung und für statische und zyklische Versuche (Spannungsverhältnisse $R = 0{\cdot}2$ und -1) bei einer einzelnen Maximalspannung verwendet. Ausgehend von diesen experimentellen Daten kann die modifizierte Spannungs-Lebensdauer Kurve (σ–t_f) und die Rißausbreitungscharakteristik (da/dt–K_I Kurve) berechnet werden, indem beides, sowohl Bruchmechanik als auch statistische Modelle, herangezogen werden. Es wurde festgestellt, daß die gemessene Versagensdauer bei zyklischer Beanspruchung, insbesondere bei dem Spannungsverhältnis -1, weitaus geringer ist als bei statischer Belastung. Das Rißwachstum bei natürlichen Fehlern kann mit Hilfe des Potenzgesetzes $da/dt = AK_I^n$ beschrieben werden. Die Ausbreitungsgeschwindigkeit von Ermüdungsrissen unter zyklischen Belastungen ist sehr viel größer als unter statischer Belastung bei gleicher Spannungsintensität. Zusammenfassend kann für die untersuchten 2Y–TZP Werkstoffe ein signifikanter Effekt zyklischer Beanspruchung festgestellt werden. Neben diesem Effekt wird bei nicht versagten Proben sowohl für statische als auch für zyklische Beanspruchung Verfestigung beobachtet. Dieser Effekt wird auf eine Veränderung der ursprünglichen Defekte während der Langzeitermüdung zurückgeführt.

Les propriétés de résistance à la fatigue statique et cyclique de deux céramiques 2Y-TZP ayant des dimensions de grain de 0·2 et 1·6 μm en moyenne ont été étudiées par flexion. Un grand nombre d'échantillons présentant des défauts naturels a été utilisé pour les mesures de la distribution initiale des containtes et pour estimer la résistance à la fatigue statique et cyclique (taux de contrainte $R = 0{\cdot}2$ et -1) et ce pour un seul niveau de contrainte maximale. De ces données expérimentales, la courbe modifiée de la durée de vie en fonction de la contrainte (σ–t_f) et la relation de propagation des fissures (courbe da/dt–K_I) peuvent être calculées en utilisant la mécanique de la rupture et les approches statistiques. Il apparait que le temps mesuré jusqu'à la fracture sous des charges cycliques, et plus particulièrement avec un taux de contrainte de -1, est beaucoup plus court que sous des charges statiques. La relation de propagation de fissures pour des défauts naturels peut être décrite par l'équation $da/dt = AK_I^n$. Les vitesses des fissures de fatigue cyclique sont beaucoup plus

* Present address: Department of Mechanical Engineering, University of Sydney, New South Wales 2006, Australia.

Journal of the European Ceramic Society 0955-2219/93/$6.00

élevées que dans le cas de charges statiques, utilisant une intensité de contrainte identique. On peut donc conclure que l'effet d'une fatigue cyclique est significatif pour des matériaux 2Y-TZP. En outre, nous avons également observé un effet de renforcement dans les échantillons ayant survécu aux tests statiques et cycliques. Ce renforcement est attribué à une modification des défauts initiaux en raison de la longue durée de mise en charge pendant les tests.

1 Introduction

Cyclic fatigue of advanced ceramic materials has recently attracted increasing attention. Fatigue crack propagation as observed on long macrocracks in Mg-PSZ,[1,2] alumina[3,4] and Ce-TZP[5] ceramics has been studied showing significant cyclic fatigue effects. For example, fatigue thresholds are found to be as low as 50% of the fracture toughness K_{IC} for Mg-PSZ and the velocities of cyclic fatigue cracks can exceed those under static fatigue loading at the same stress intensity by orders of magnitude.

The extrapolation of such fatigue results with long cracks to the fatigue properties of ceramics with small or even processing flaws may be critical because of the so-called 'small crack effect' both in the R curve behaviour and in the fatigue properties. For example, the R curve measured with small cracks can be much lower than that with long cracks for Al_2O_3[6] and for Mg-PSZ,[7] and the fatigue crack propagation of small cracks can occur at stress intensities far below the threshold values derived from long cracks.[8] On the other hand, ceramic materials cannot tolerate long cracks in their application simply because of the low resulting strength. It is therefore very important to understand the fatigue behaviour of ceramic materials with processing flaws.

Static and cyclic fatigue behaviour of Mg-PSZ,[8,9] Y-TZP(A)[10] and Ce-TZP[11] ceramics with natural flaws was also investigated revealing significant cyclic fatigue effects. Fatigue life time under cyclic loading can be more than three orders of magnitude shorter than under static loadings at the same stress levels. In this paper the static and cyclic fatigue of two 2Y-TZP materials with processing flaws was investigated using both fracture mechanics and statistical methods. The modified stress–life time curves and the da/dt–K_I curves were calculated.

2 Experimental Procedures

2.1 Materials

Commercial ZrO_2 powder containing 2 mol% Y_2O_3 (TZ-2Y) (Tosoh Corp., Tokyo, Japan) was used for this investigation. The received powder was first compacted with a uniaxial die at 6 MPa followed by isostatic pressing at 400 MPa. In order to obtain different grain sizes, the green compacts were sintered at temperatures of 1400 and 1600°C for 0·5 and 10 h, respectively. From the sintered plates, bend specimens $3{\cdot}5 \times 4{\cdot}5 \times 45\,mm^3$ were cut and ground with diamond tools. In the mechanical tests, the specimens generally fail due to inherent flaws (sintering flaws) and not to flaws introduced by machining. For releasing the residual stresses after machining the specimens were subjected to heat treatment at 1350°C for 2 h in air.

The materials were characterized in their phase composition by an X-ray diffraction technique and by SEM examination on both polished and fracture surfaces. Densities were measured by the water displacement technique. A four-point loading fixture with 20 and 40 mm as inner and outer span widths, respectively, was used to determine the inert bending strength in air with a loading rate of 1000 N/s. The fracture toughness K_{IC} was measured by the bridge method described elsewhere.[12]

2.2 Fatigue experiments

Static fatigue experiments were performed as four-point bending tests in air at about 20°C with a fixed

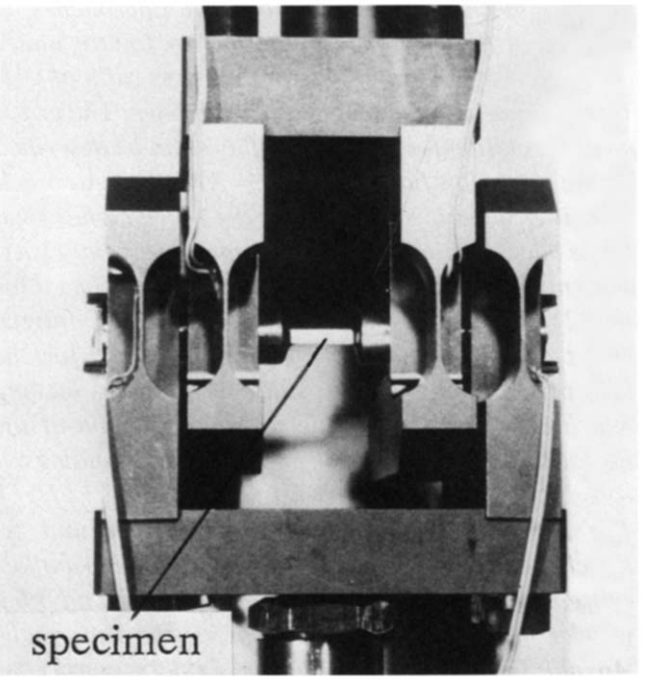

Fig. 1. Loading arrangement (a) and specimen (b) for the cyclic fatigue tests with the stress ratio $R = -1$.

Table 1. Sintering conditions, average grain sizes, densities and ZrO_2-phase analysis

Material	*Sintering conditions*	*Grain size* (μm)	*Density* (*% TD*)	$\frac{m}{m+t+c}$ (%)		
				Sintered surface	*Ground surface*	*Fracture surface*
2Y-TZP-I	1400°C, 0·5 h	0·2	99·7	0	9	45
2Y-TZP-II	1600°C, 10 h	1·6	96·4	5	25	50

TD = Theoretical density.

maximal duration of loading of 400 h. The cyclic fatigue tests were realized with an electromagnetic resonance machine under load control as bending tests with two stress ratios, $R = 0{\cdot}2$ and -1. The frequency was kept constant at 70 Hz. While a four-point bending fixture was used for the cyclic fatigue tests with the stress ratio of 0·2, a special fixture, as shown in Fig. 1(a), was used for the cyclic fatigue tests with the stress ratio of -1. In this case the bending specimen ($3{\cdot}5 \times 4{\cdot}5 \times 45\,mm^3$) was fixed into two brass cylinders with a special mixture of adhesive with B_4C powder, as shown in Fig. 1(b). The outer fibre stress of the bending specimens was determined from the signals of strain gauges attached both on the tensile and compression surfaces of each individual bending specimen. As for the Weibull distribution of the inert strength, 24 specimens were tested for each individual set of loading conditions.

3 Results and Analysis

3.1 Material characterization

Table 1 shows the sintering conditions, grain size and achieved densities as well as the amount of the monoclinic phase in different states of the materials. The lower density achieved at the higher sintering temperature and longer sintering time may be caused by the so-called 'swell effect' occurring at higher sintering temperatures.[13] With increasing grain size the amount of the stress-induced t–m transformation is increased in all investigated states of the surfaces, i.e. sintered, ground and fracture surfaces. The mechanical properties are listed in Table 2. The lower density of the 2Y-TZP-II material leads to a marked decrease of the Vickers hardness, Young's modulus as well as of flexural strength and fracture toughness. Figure 2 shows the Weibull distribution of the inert bending strength data for the two materials with natural flaws. The Weibull parameters for the two materials are:

$$\sigma_0 = 931\,MPa;\ m = 9{\cdot}8 \quad \text{for 2Y-TZP-I}$$
$$\sigma_0 = 548\,MPa;\ m = 8{\cdot}8 \quad \text{for 2Y-TZP-II}$$

3.2 Fatigue behaviour

Table 3 shows the stress levels and the number of the initial fractures (i), the fatigue fractures (f) and the survivors (s) under both, static and cyclic (stress ratios $R = 0{\cdot}2$ and -1) loading conditions. Although the stress levels under static loading are much higher than under cyclic loadings, the number of survivor specimens under static loading is almost the same as under cyclic loading with stress ratio of 0·2. Under cyclic loading with the stress ratio of -1 most specimens failed during the fatigue test at the same (as for 2Y-TZP-I) or even lower (as for 2Y-TZP-II) stress levels compared to that with the stress ratio of 0·2. This indicates the cyclic fatigue damage is more pronounced at the stress ratio of -1.

Table 3 also contains values of the life time and number of cycles to failure at the failure probability of 50%; the complete Weibull distributions of the failure probabilities as a function of the life time under both static and cyclic loadings are represented in Fig. 3. The specimens fractured during the fatigue tests are displayed here with their corresponding failure probabilities as being determined on the basis of the sample size of 24 specimens; the spontaneously failed and the survivor specimens (not shown in Fig. 3) are correlated with the lower and the higher failure probabilities, respectively, compared to the specimens failed during fatigue testing. Despite the higher stress levels under static loading the longest time to failure at the same failure

Table 2. Mechanical properties of ZrO_2 ceramics

Material	*Vickers hardness*	*Young's modulus* (*GPa*)	*Modulus of rupture* (*MPa*)	*Fracture toughness* ($MPa\,m^{0.5}$)
2Y-TZP-I	1 260	205	882 ± 118	5·1
2Y-TZP-II	800	174	520 ± 67	4·6

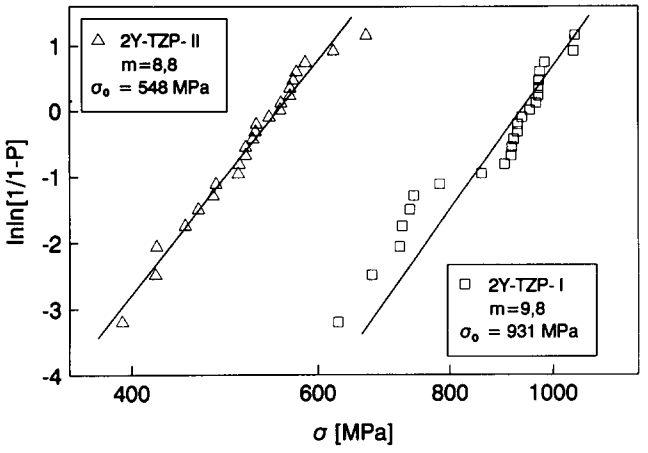

Fig. 2. Weibull distribution of the inert strength of 2Y-TZP ceramics.

probability was measured under static loading and the shortest time to failure was measured under cyclic loading with the stress ratio of -1. From the experimental data in Fig. 3 the Weibull parameter m^* for the life time distribution as formulated in the following equation:

$$\ln \ln \frac{1}{1-P} = m^* \ln t_f + m^* \ln c \qquad (1)$$

can be calculated[14,15] (see Appendix 1) using the so-called maximum likelihood method.[16] From these m^* values the n values in the power law function for the crack propagation:

$$\frac{da}{dt} = AK_I^n \qquad (2)$$

can be calculated from the equation:

$$m^* = \frac{m}{n-2} \qquad (3)$$

where m is the Weibull parameter of the initial inert strength distribution.

The modified stress–life time (σ–t_f) curves of both materials are shown in Fig. 4. For this purpose the stress/inert strength ratio σ/σ_c was calculated using the applied stress in the fatigue tests (static stress and maximum stress in the static and cyclic tests, respectively) and relating it to the Weibull distribution of the inert strength of the materials. In Fig. 4 only the specimens which failed during the fatigue tests are considered (see also Table 3); their fatigue stress is correlated to the inert strength of the individual specimens (Fig. 2) with the same failure probability. Here it is assumed that the four material series A, B, C and D for the strength measurement,

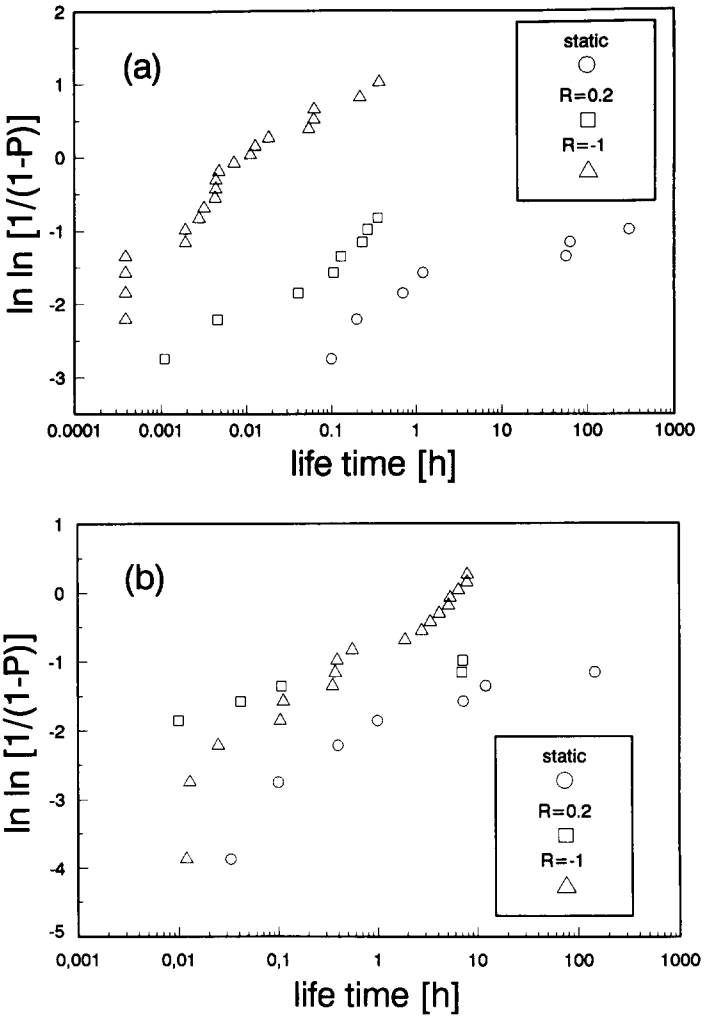

Fig. 3. Weibull distributions of the life time under static and cyclic loadings for (a) 2Y-TZP-I and (b) 2Y-TZP-II materials. For loading conditions see Table 3.

Table 3. Compilation of experimental fatigue data. Number of specimens (i) failed during the first loading cycle, (f) failed during the fatigue test, (s) not failed after the limit number of cycles

Material	*Loading conditions*	*Stress (MPa)*	*Number of specimens*			*Life time at P = 50% (h)*	*No. of cycles at P = 50%*
			i	*f*	*s*		
2Y-TZP-I	Static	$\sigma_s = 690$	1	7	15	6769	—
	Cyclic; $R = 0{\cdot}2$	$\sigma_{max} = 600$	1	8	15	63	15876000
	Cyclic; $R = -1$	$\sigma_{max} = 600$	2	21	0	0·0045	1134
2Y-TZP-II	Static	$\sigma_s = 450$	0	7	17	11407	—
	Cyclic; $R = 0{\cdot}2$	$\sigma_{max} = 400$	3	5	16	3204	807410000
	Cyclic; $R = -1$	$\sigma_{max} = 350$	0	18	6	2·28	574560

P = Failure probability (see eqn (1)).
σ_s = Constant stress.

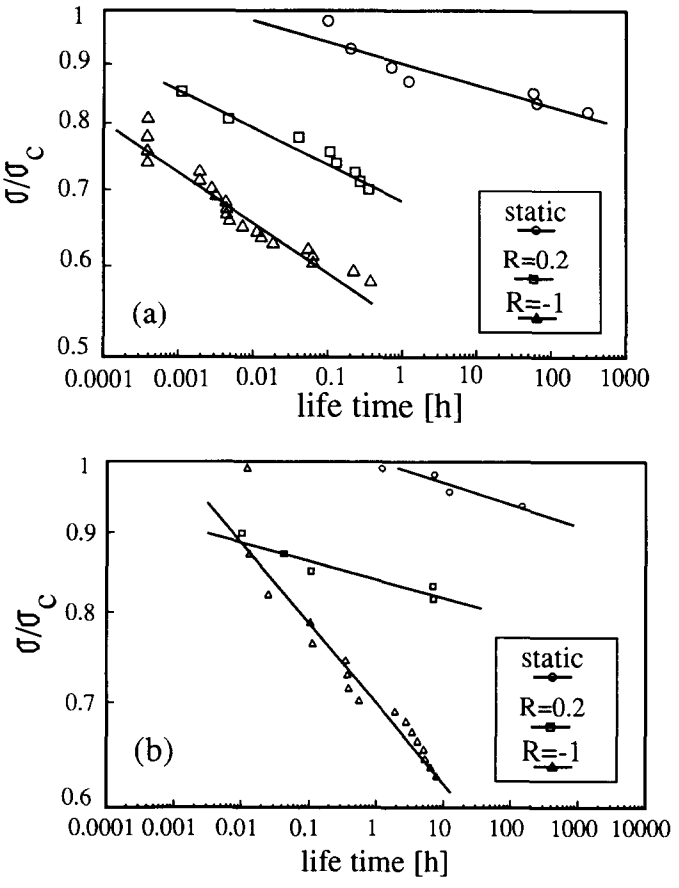

Fig. 4. Modified stress–life time (σ–t_f) curves under static and cyclic loadings for (a) 2Y-TZP-I and (b) 2Y-TZP-II materials. For loading conditions see Table 3.

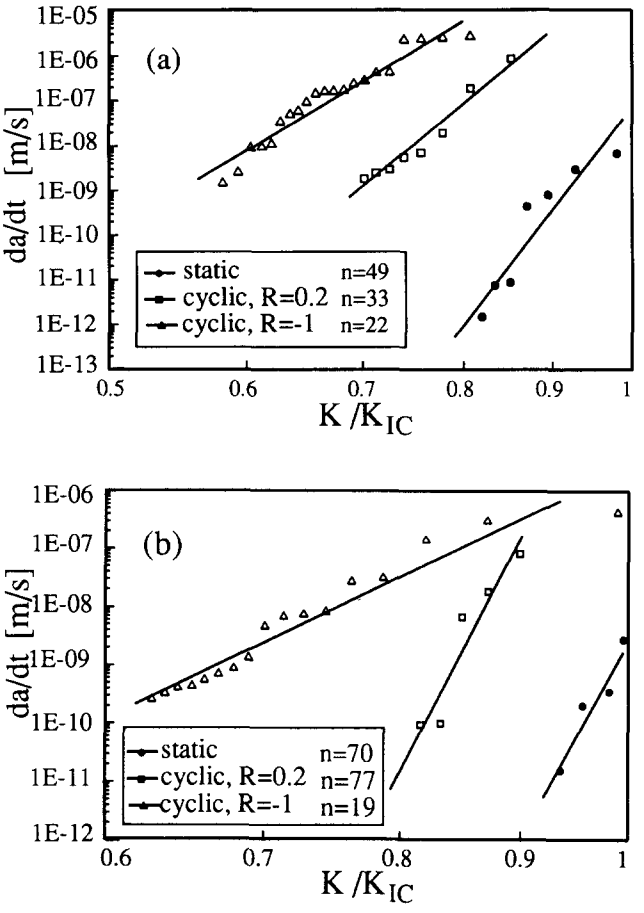

Fig. 5. Crack propagation curves under static and cyclic loadings with natural flaws: (a) 2Y-TZP-I, (b) 2Y-TZP-II.

for the static and for both cyclic fatigue tests, respectively, are equivalent with respect to their distributions of the initial flaws so that the initial strength can be described by the same Weibull distribution and the same Weibull parameters. The n values can also be calculated from the slope in the $\ln\sigma$–$\ln t_f$ plot, where the slope is equal to $-1/n$ (see Appendix 1). The n values are listed in Table 4 and compared with the results obtained through other methods.

The crack growth relation can also be calculated from the experimental data of the fatigue and the initial strength distributions by the so-called statistical method[17] (see Appendix 2). The da/dt–K_I curves are shown in Fig. 5. The relationship between the crack growth rate and the stress intensity factor K_I can be represented as a power law function as shown in eqn (2). The n values derived from this method for the two materials under static and cyclic loadings are also shown in Table 4 and compared with those from the other methods. It can be seen that the n values under cyclic loading, especially with stress ratio of -1, are much lower than under static loading.

The residual strengths of the survivor specimens were also measured after the fatigue tests. The results are represented together with the Weibull distribution of the initial strength in Fig. 6. Necessarily, the residual strength values appear as truncated strength distributions. They are compared with the corresponding initial strength values with the highest failure probabilities since it can be conjectured that these survivor specimens would have had a higher failure probability in their initial

Table 4. Comparison of the n values determined by different methods

2Y-TZP-I			*2Y-TZP-II*			*Method*
Static loading	*Cyclic loading, R = 0·2*	*Cyclic loading, R = −1*	*Static loading*	*Cyclic loading, R = 0·2*	*Cyclic loading, R = −1*	
59	58	26	46	96	19	$m^* = m/(n-2)$
54	32	23	73	83	19	Slope: $-1/n$
49	33	22	70	77	19	Statistic

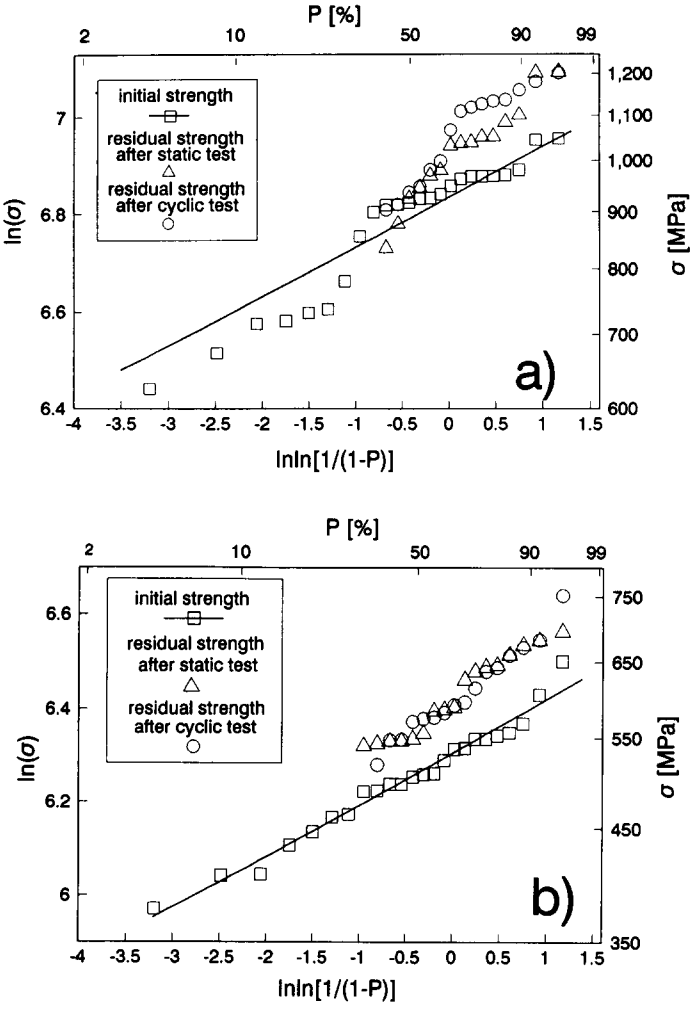

Fig. 6. Weibull distributions of initial strength, residual strength of survivor specimens after static ($t_L = 400$ h) and cyclic ($R = 0{\cdot}2, f = 70$ Hz, $N_L = 2 \times 10^6$) loadings: (a) 2Y-TZP-I, (b) 2Y-TZP-II.

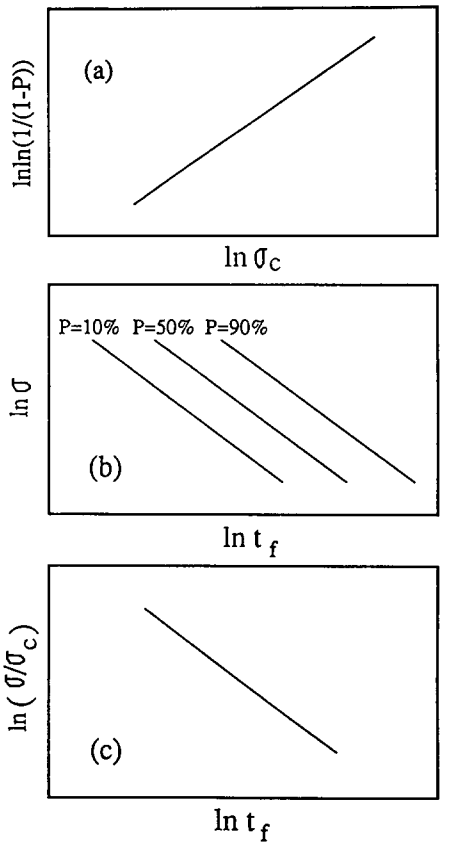

Fig. 7. Correlation between the Weibull distribution of the initial strength (a), the 'conventional' s/t curve (b) and the 'modified' σ–t_f curve (c).

state than the specimens which failed during the fatigue tests. As shown in Fig. 6, the residual strength of the survivor specimens after long term fatigue tests is clearly higher than the initial strength. Table 5 shows the amount of the stress-induced t–m transformation at the fracture surfaces by the strength measurement and by the static and cyclic fatigue tests. With increasing grain size the amount of the t–m transformation is increased, although the flexural strength of 2Y-TZP-II material is much lower than for the 2Y-TZP-I material. Moreover, the fatigue specimens showed lower amount of phase transformation on the fracture surface than that by the strength measurement, which is caused by the lower stress levels of the static and cyclic fatigue tests.

4 Discussion

The modified σ–t_f curve represented in this paper (Fig. 4) provides a new effective method to evaluate the dependence of the life time on the fatigue stress levels (so-called s/N or s/t curve) from the Weibull distribution of the initial strength and from the fatigue data measured at a single stress level. In the 'conventional' s/N or s/t curve the constant flaw size expressed as a particular failure probability leads to a distribution of the life time with changing fatigue stress levels, as shown schematically in Fig. 7(b). This means nothing else than the dependence of the life time on the fatigue stress levels for a certain flaw size which can be represented at constant failure

Table 5. Stress-induced t–m transformation at the fracture surfaces after different loading experiments (% monoclinic ZrO_2 phase)

Material	*Strength measurement*	*Static fatigue*	*Cyclic fatigue, $R = 0{\cdot}2$*	*Cyclic fatigue, $R = -1$*
2Y-TZP-I	44·5	41·2	41·2	39·6
2Y-TZP-II	50·3	42·7	42·2	41·5

probabilities (for example 10, 50 or 90% in the distribution of either initial strength or life time in the fatigue tests). For ceramic materials a large number of specimens at each fatigue stress level must be used in order to obtain a s/N or s/t curve with acceptable statistical accuracy.

In the modified (σ–t_f) curve as shown schematically in Fig. 7(c), however, only two series of specimens are needed with one series for the initial strength distribution (Fig. 7(a)) and the other series for the fatigue tests at a single stress level. Here the stress in the fatigue test is chosen at one level but the flaw sizes of the specimens are naturally changing which can be evaluated from the Weibull distribution of the initial strength. The prerequisite for this method is the assumption of the same distribution of the flaw size and the initial strength for both series of specimens, which can be fulfilled by testing a large number of specimens in both the inert strength measurement and the fatigue test.

These two approaches for obtaining s/t or s/N curves, namely the change of stress levels for constant flaw sizes, i.e. failure probabilities, and the change of flaw sizes at constant stress levels, can be regarded as equivalent and can even be converted into each other. For a particular σ_c value with a corresponding failure probability which can be calculated from the Weibull distribution of the initial strength, the modified σ–t_f curve can then be transferred to the 'conventional' s/t curve by substituting this σ_c value into the σ/σ_c. The σ–t_f curve obtained in this way represents then the dependence of the life time on the stress levels at a failure probability which is equal to the failure probability of the σ_c. By repeating this process with different σ_c values and their corresponding failure probabilities, the dependence of the life time on the stress levels at different failure probabilities, i.e. the 'conventional' s/t curve, can then be evaluated. Figure 8 shows the 'conventional' s/t curves under static and cyclic loadings for the 2Y-TZP-I material at the failure probabilities of 10, 50 and 90%, respectively, which are calculated from the data in Fig. 3. The measured life time under cyclic loading, especially with the stress ratio of -1, is much lower than under static loading, from which the marked cyclic fatigue effect can again be concluded.

The 2Y-TZP materials investigated here showed both static and cyclic fatigue effects; the latter can be clearly seen in the shorter life time at the same stress levels or in the higher crack velocities at the same stress intensity factors. This cyclic fatigue effect may be caused by effects of 'microplasticity' due to the stress-induced t–m transformation around the initial flaws. On the other hand, a strengthening effect was also observed by the survivor specimens after long term static and cyclic loadings. These weakening

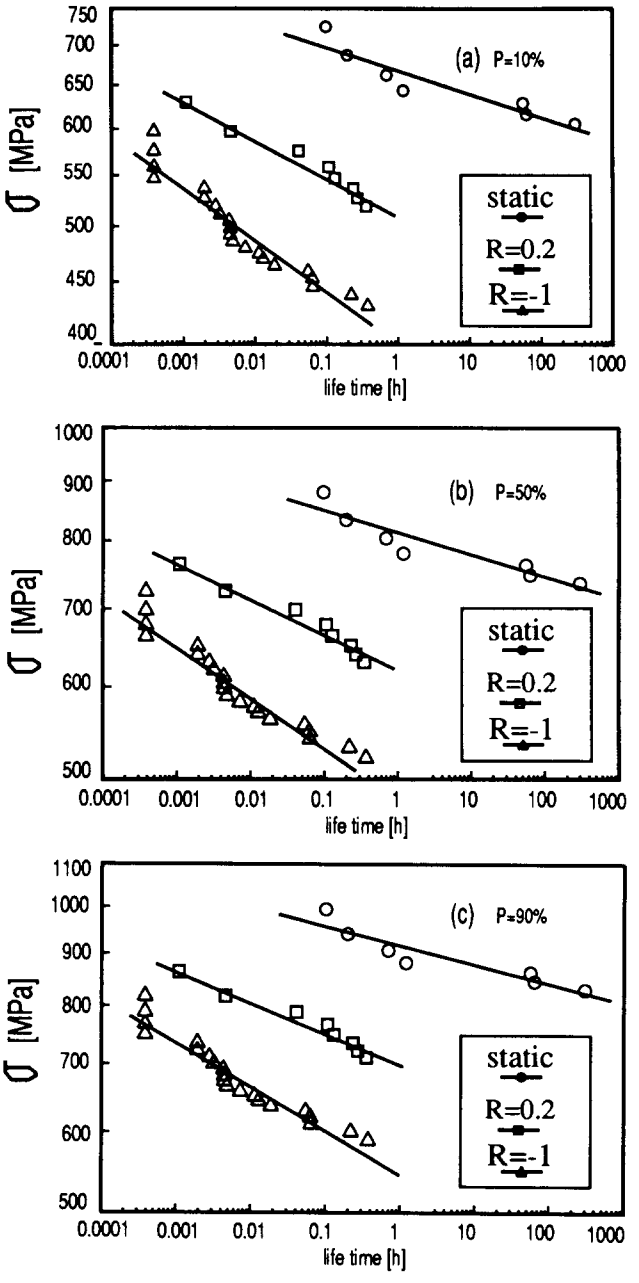

Fig. 8. Converted s/t curves of the 2Y-TZP-I material at the failure probabilities of 10, 50 and 90%.

(static and cyclic fatigue) and strengthening effects during the long term mechanical loadings are accompanied by a very interesting dependence of the change of the microstructure on the loading time. Under long term static or cyclic loadings at K_I values lower than the K_{IC} value, the microstructure around the initial flaws can be changed. For example, stress-induced t–m transformation can occur, the residual stress can be changed and the geometry of the flaw can be modified. In their early stage these processes can lead to an increase of the residual strength of the materials. However, if the time or cycles of loading are further increased cracks will begin to propagate and fatigue effects can be then observed. Indeed, the change of the flaw characteristics during fatigue loading should be investigated further.

The n values for the crack propagation relations

derived from the three methods showed slight differences. These three methods are used without any special assumptions: no R curve behaviour and no cyclic fatigue effect are considered or presumed, and therefore they should give the same n values. The differences in the n values from the three methods may become smaller when a higher number of fatigue specimens especially under static and cyclic loading with stress ratio of 0·2 could be tested. Nevertheless, the lower n values under cyclic loading, especially with stress ratio of -1, again indicate the special cyclic fatigue effect. The crack propagation relations under cyclic loadings should be investigated more intensively in the future, from which the life time under cyclic loadings can then be predicted.

5 Conclusion

2Y-TZP materials showed both static and cyclic fatigue effects; the latter can be seen in the shorter life time and higher crack velocities under cyclic loadings compared with that under static loadings at the same stress (σ) or stress intensity (K_I) levels.

Besides these static and cyclic fatigue effects, a strengthening effect can also be observed by the survivor specimens after long term loadings. Both the weakening and the strengthening effects during the long term loadings indicate the change of the microstructure around the initial flaws and their time dependence.

The crack propagation relations under static and cyclic loadings can be described by the power law function $da/dt = AK_I^n$. The n values can be derived from the Weibull distribution of the life time, from the modified σ–t_f curve and from the 'statistical method'. Under static loadings the n values are much higher than under cyclic loadings.

Stress-induced t–m transformation at the fracture surfaces in the 2Y-TZP materials depends not only on the grain size but also on the applied stress levels.

References

1. Dauskardt, R. H., Yu, W. & Ritchie, R. O., Fatigue crack propagation in transformation-toughened zirconia ceramic. *J. Am. Ceram. Soc.*, **70** (1987) C248–52.
2. Dauskardt, R. H., Marshall, D. B. & Ritchie, R., Cyclic fatigue-crack propagation in magnesia-partially-stabilized zirconia ceramics. *J. Am. Ceram. Soc.*, **73** (1990) 893–903.
3. Lathabai, S., Roedel, J. & Lawn, B., Cyclic fatigue from frictional degradation at bridging grains in alumina. *J. Am. Ceram. Soc.*, **74** (1991) 1340–8.
4. Guiu, F., Reece, M. J. & Vaughan, D. A. J., Static and cyclic fatigue in some structural ceramics. In *Structural Ceramics, Processing, Microstructure and Properties*, ed. J. J. Bentzen, J. B. Bilde-Sorensen, N. Christiansen & B. Ralph. 11th RISO Int. Symp. on Metallurgy and Materials Science, 1990, Riso National Laboratory, Roskilde, Denmark, pp. 313–18.
5. Tsai, J.-F., Yu, C.-S. & Shetty, D. K., Fatigue crack propagation in ceria-partially-stabilized zirconia (Ce-TZP)-alumina composites. *J. Am. Ceram. Soc.*, **73** (1990) 2992–3001.
6. Steinbrech, R. W. & Schmenkel, O., Crack-resistance curves of surface cracks in alumina. *J. Am. Ceram. Soc.*, **71** (1988) C271–3.
7. Marshall, D. B. & Swain, M. V., Crack resistance curves in magnesia-partially-stabilized zirconia. *J. Am. Ceram. Soc.*, **71** (1988) 399–407.
8. Swain, M. V. & Zelizko, V., Comparison of static and cyclic fatigue on Mg-PSZ alloys. In *Advances in Ceramics, Vol. 24, Science and Technology of Zirconia III*. American Ceramic Society, Westerville, OH, 1988, pp. 595–606.
9. Bowman, K. J., Morel, P. E. R. & Chen, I.-W., Reversible transformation plasticity in uniaxial tension-compression cycling of Mg-PSZ. *Mat. Res. Soc. Symp. Proc.*, **78** (1986) 51–8.
10. Grathwohl, G. & Liu, T., Crack resistance and fatigue of transforming ceramics: I, Materials in the ZrO_2–Y_2O_3–Al_2O_3 system. *J. Am. Ceram. Soc.*, **74** (1991) 318–25.
11. Grathwohl, G. & Liu, T., Crack resistance and fatigue of transforming ceramics: II, CeO_2-stabilized tetragonal ZrO_2. *J. Am. Ceram. Soc.*, **74** (1991) 3028–34.
12. Brugger, N., Crack behaviour in ceramic materials under static, slowly increasing and cyclic loading conditions. Doctoral thesis, University Karlsruhe, Karlsruhe, Germany 1986 (in German).
13. Liu, T. & Dorfschmidt, K, Sintering behaviour and optimization of partially stabilised ZrO_2. Annual Meeting DKG, Munich, Germany, 18–20 Oct. 1988 (in German).
14. Evans, A. G. & Fuller, E. F., Crack propagation in ceramic materials under cyclic loading conditions. *Metallurgical Transactions*, **5** (Jan) (1974) 27–33.
15. Hu, X. Z., Mai, Y.-W. & Cotterell, B., A statistical theory of time-dependent fracture of brittle materials. *Philosophical Magazine A*, **58**(2) (1988) 299–324.
16. Harter, H. L. & Moore, A. H., Maximum-likelihood estimation of the parameters of gamma and Weibull populations from complete and from censored data. *Technometrics*, 7 (1965) 639–43.
17. Fett, T. & Munz, D., Determination of v–K_I-curves by a modified evaluation of lifetime measurements in static bending tests. *Commun. Am. Ceram. Soc.*, **68** (1985) C213–15.
18. Ritter, J. T., Jr., Engineering design and fatigue failure of brittle materials. In *Fracture Mechanics of Ceramics, Vol. 4, Crack Growth and Microstructure*, ed. R. C. Bradt, D. P. H. Hasselmann & F. F. Lange. Plenum Press, New York, 1978, pp. 667–86.

Appendix 1: Life Time Prediction Based on Weibull Statistics and Fracture Mechanics[14,15]

The slow crack growth in ceramic materials can be described by the power law function:

$$\frac{da}{dt} = AK_I^n \tag{A1}$$

where da/dt is the crack velocity, K_I is the applied crack-tip stress intensity factor, and (A, n) are numerical constants depending on the particular material-environment system. Applying the general condition:

$$K_I = Y\sigma_a a^{1/2} \tag{A2}$$

where σ_a is the applied stress and Y is a geometrical factor, and substituting for K_I in eqn (A1) gives:

$$a^{-n/2}\frac{da}{dt} = AY^n\sigma_a^n \tag{A3}$$

Integrating eqn (A3) to obtain the crack growth in time, t, gives:

$$\int_{a_i}^{a_c} a^{-n/2}\,da = \int_0^{t_f} A(\sigma_a Y)^n\,dt \tag{A4}$$

where a_i is the initial crack length, a_c is the crack length at fatigue time t_f, so that:

$$A(\sigma_a Y)^n t_f = \frac{2}{2-n}\left(a_c^{(2-n)/2} - a_i^{(2-n)/2}\right) \tag{A5}$$

Substituting the following equations:

$$a_c = \left(\frac{K_{IC}}{\sigma_a Y}\right)^2 \tag{A6}$$

and

$$a_i = \left(\frac{K_{IC}}{\sigma_i Y}\right)^2 \tag{A7}$$

into eqn (A5) one obtains:

$$A\sigma_a^n Y^n t_f = \frac{2}{2-n}\left[\left(\frac{\sigma_a Y}{K_{IC}}\right)^{n-2} - \left(\frac{\sigma_i Y}{K_{IC}}\right)^{n-2}\right] \tag{A8}$$

Since $n \gg 2$ for ceramic materials, eqn (A8) can be rewritten as:

$$t_f\sigma_a^n = \frac{2\sigma_i^{n-2}}{(n-2)AY^2K_{IC}^{n-2}} \tag{A9}$$

From the Weibull distribution of the initial strength σ_i:

$$\ln\ln\frac{1}{1-P} = m\ln\left(\frac{\sigma_i}{\sigma_0}\right) \tag{A10}$$

one obtains:

$$t_f\sigma_a^n = \frac{2\sigma_0^{n-2}\left(\ln\dfrac{1}{1-P}\right)^{(n-2)/m}}{(n-2)AY^2K_{IC}^{n-2}} \tag{A11}$$

For a constant applied stress σ_a, eqn (A11) can be rewritten as:

$$\ln\ln\frac{1}{1-P} = m^*\ln t_f + m^*\ln c \tag{A12}$$

where

$$m^* = \frac{m}{n-2} \tag{A13}$$

and

$$c = \frac{(n-2)AY^2K_{IC}^{(n-2)}\sigma_a^n}{2\sigma_0^{n-2}} \tag{A14}$$

and for a particular failure probability P, eqn (A11) can be rewitten as:

$$\ln\sigma_a = -\frac{1}{n}\ln t_f + \frac{1}{n}\ln B \tag{A15}$$

with

$$B = \frac{2\sigma_0^{n-2}\left(\ln\dfrac{1}{1-P}\right)^{(n-2)/m}}{(n-2)AY^2K_{IC}^{n-2}} \tag{A16}$$

Appendix 2: Statistical Method for Determination of da/dt_f Curve with Natural Flaws[17]

The velocity of subcritical crack growth is usually related to the stress intensity factor K_I:

$$\frac{da}{dt} = v(K_I) \tag{A17}$$

If a is the size of a surface crack, the stress intensity factor is given by:

$$K_I = \sigma_a a^{1/2} Y \tag{A18}$$

where σ_a is the applied stress and Y is the geometrical factor. The life time of a specimen containing a crack of initial crack size a_i and loaded by stress σ_a is given by:[18]

$$t_f = \frac{2}{Y^2\sigma_a^2}\int_{K_{Ii}}^{K_{IC}} \frac{K_I}{v(K_I)}\,dK_I \tag{A19}$$

where

$$K_{Ii} = \sigma_a a_i^{1/2} Y \tag{A20}$$

is the initial value of the stress intensity factor. By differentiation of eqn (A19) with respect to the initial stress intensity factor K_{Ii}, one obtains:

$$\left.\frac{dt}{dK_{Ii}}\right|_{\sigma_a = \text{constant}} = -\frac{2K_{Ii}}{Y^2\sigma_a^2 v(K_{Ii})} \tag{A21}$$

Use of the logarithmic derivations:

$$t_f d(\ln t_f) = dt_f \tag{A22}$$

and

$$K_{Ii}\,d(\ln K_{Ii}) = dK_{Ii} \tag{A23}$$

yields:

$$\frac{d(\ln t_f)}{d(\ln K_{Ii})} = -\frac{2K_{Ii}^2}{Y^2\sigma_a^2 t_f v(K_{Ii})} \tag{A24}$$

and, consequently, the crack growth rate belonging to K_{Ii} becomes:

$$v(K_{Ii}) = -\frac{2K_{Ii}^2}{Y^2\sigma_a^2 t_f}\frac{d(\ln K_{Ii})}{d(\ln t_f)} \tag{A25}$$

Since:

$$\frac{K_{Ii}}{K_{Ic}} = \frac{\sigma_a}{\sigma_c} \tag{A26}$$

eqn (A25) becomes:

$$v\left(\frac{K_{Ii}}{K_{Ic}}\right) = -\frac{2K_{Ic}}{Y^2\sigma_c^2 t_f}\frac{d\left(\ln\dfrac{K_{Ii}}{K_{Ic}}\right)}{d(\ln t_f)} \tag{A27}$$